Development of a Non-Cloggable Subsea Data Logger for Harsh Turbidity Current Monitoring

Luke J. Bradley, Sean C. Ruffell, Peter J. Talling and Nick G. Wright *Member, IEEE*

***Abstract*—Large submarine flows of sediment (sand and mud), known as turbidity currents, transfer and bury significant amounts of organic carbon and pollutants to the deep sea via submarine canyons. They are also significant geohazards, regularly breaking networks of seabed telecommunications cables that carry $>$ 99% of global data that underpin the internet. Despite this, key parameters (notably their sediment concentration) in these flows are yet to be directly measured in real-time due to their inherently harsh environment that is unsuitable for commercial conductivity sensors. To address this issue, a subsea datalogger (SSDL) is developed with a planar conductivity sensor head that can measure the sediment concentration within dense turbidity currents. Unlike conventional sensors, the planar design of the SSDL's sensor prevents clogging at high sediment concentrations, allowing for continuous measurements within turbidity currents. The conductivity sensor is developed with a temperature sensor which is measured using an external 16-Bit ADC which is controlled with a SAMD21 32-Bit ARM microcontroller. The SSDL measures the temperature and the conductivity of the seawater once every 4 seconds for over a year. In an initial device test, the SSDL can record a turbidity current within the Bute Inlet, Canada. It is found that the seawater's conductivity increases with salinity concentration and decreases with sediment concentration. The SSDL developed here can thus be used for both conventional subsea datalogging applications and high turbidity current applications.**

***Index Terms*—Turbidity current, salinity, sediment concentration, data logger**

I. Introduction

Turbidity currents are density driven, seafloor hugging gravity flows that transport large quantities of sediment to the deep sea via submarine canyons, making them volumetrically one of the most important sediment transport process on our planet. A single turbidity current can transport over ten times the annual flux of all the worlds' rivers [1]. They are responsible for the transport of organic carbon [2] and micro plastics [3] [4] to the deep ocean, as well as nutrients that support unique ecosystems in and around submarine canyons. It is important to investigate these flows as they pose major hazards to seafloor infrastructure including seafloor pipelines and telecommunication cables that transmit 99% of global data traffic [5]. A key remaining question is whether these flows are dilute sediment suspensions or contain a dense layer at their base with very different physics. In order to characterise the flows of turbidity currents, a sensor must be developed that can record the sediment concentration for the entire duration of the event.

Within literature, multiple methods for measuring the sediment concentration within the ocean have been demonstrated. Such efforts include satellite sensing [6], [7] where multiple sensors transfer all the data back to a master controller. Other methods utilise RFID tags [8] but suffer from poor resolution and high power consumption. The most conventional method for measuring high turbid water flows are optical sensors due to their high accuracy [9], [10]. Despite their accuracy, these optical sensors require significant calibration to correct for particle size and density and cannot be used to measure high sediment concentrations due to sensor saturation [11]. A planar conductivity concentration profiler was presented in [12] which has been widely used in similar works for measuring sediment concentration [13], [14]. Despite the small profile and planar transformer, the system uses multiple sensing channels which will minimise battery lifetime and cannot be left to operate remotely for long periods of time. As well as this, the profilers use gold plated contact during measurements that will slowly corrode over time and are not suited for the time periods associated with turbidity currents [12].

Here, a new conductivity sensor consisting of a platinum electrode sensor head is presented. By using a planar conductivity sensor head, it is possible to measure the seawater's sediment concentration without the need for a protruding geometry, thus preventing clogging. The drawback of a planar design is that the seawater's conductivity cannot be calculated as the sensor dimensions are unknown. To alleviate this, the conductivity sensor is calibrated based on temperature and salinity concentration before being deployed.

The SSDL was tested and calibrated within a laboratory environment using water with different salinity concentrations. Following testing and calibration, the sensor was deployed in Bute Inlet, BC, Canada, where it was able to monitor the suspended sediment concentrations within a turbidity current. Unlike previous dataloggers, the SSDL developed here does not show any issues with clogging at high sediment concentrations and measures a monotonic decrease in conductivity with increasing sediment concentration. The groundwork developed here provides researchers with a standard method of developing a conductivity sensor for extreme turbidity currents.

II. Sensor driving and sensing circuitry

The sensor used to measure the saline water conductivity consists of two platinum electrodes that are separated by

Luke J. Bradley (corresponding author: Luke.Bradley@strath.ac.uk) is with the Rolls Royce UTC at the University of Strathclyde, Glasgow, UK. Sean Ruffell and Peter Talling are with the Department of Earth Science at Durham University, Durham, UK. Nick G. Wright is with the School of Engineering at Newcastle University, Newcastle-upon-Tyne, UK. This work was supported through the UK EPSRC Future Metrology Hub through the award EP/P006930/1.

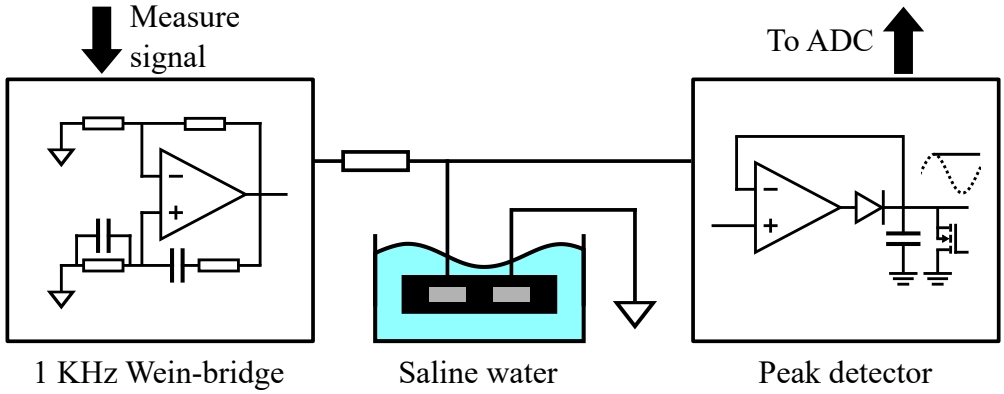

Fig. 1: Analogue circuitry consisting of the Wein-bridge oscillator and the peak detector circuit.

1 cm and are encapsulated within a carbon fibre 3D printed holder. As saline water is conductive, a DC potential divider circuit could be used to measure the conductivity, although this requires considerably low voltages to avoid electrolysis of the contacts. Here, an AC driving signal is used to drive the conductivity sensor in a potential divider configuration (Fig. 1). The AC signal generated from the Wein-bridge oscillates from 0 to 3.3 V and a 1.65 V regulator is used to generate the offset voltage for the Wein-bridge and the conductivity sensor. The AC signal over the conductivity sensor will have an output voltage given by

$$V_{out} = V_{in}\left[\frac{R_{cs}}{R + R_{cs}}\right] \tag{1}$$

where V_{in} is the amplitude of the AC signal generated from the Wein-bridge circuit, R is the series resistor used at the output of the Wein-bridge and R_{cs} is the resistance of the conductivity sensor. After driving the sensor, a peak detector circuit measures the amplitude of the output voltage. The peak detector operates through charging an output capacitor that charges to the peak of input signal. The diode ensures the capacitor remains charged after the peak of the signal and the MOSFET discharges the capacitor between measurements. The Wein-bridge generates an AC signal for a period of 50 ms before an ADC measures the voltage at the output of the peak detector. The driving and sensing circuitry contributes to the majority of the current consumption and so the driving and sensing time is limited to 50 ms to maximise battery life.

III. Control circuit

The topology for the SSDL is illustrated in Fig. 2. The SSDL logger is controlled using the Arduino MKR zero microcontroller [15]. The MKR zero board uses the SAMD21 Cortex®-M0+ 32-bit low-power ARM MCU and an SD card holder. The SAMD21 Cortex microcontroller is a 48 MHz 32-bit microcontroller with a deep sleep power mode that consumes less than 100 μA. Here, the microcontroller measures the conductivity and temperature sensors using an external 16-bit ADS1115 ADC. The temperature sensor and conductivity are measured at 4 s intervals. To reduce power consumption, the conductivity and temperature data is appended to the internal SRAM after every measurement and data is only saved to the SD card once every 4 minutes. A DS3231 precision RTC records the time of each measurement. The DS3231 RTC uses an internal temperature compensation circuitry to reduce the clock drift of the internal oscillator to less than 2 s/year. An LM35CAZ precision temperature sensor measures the water's

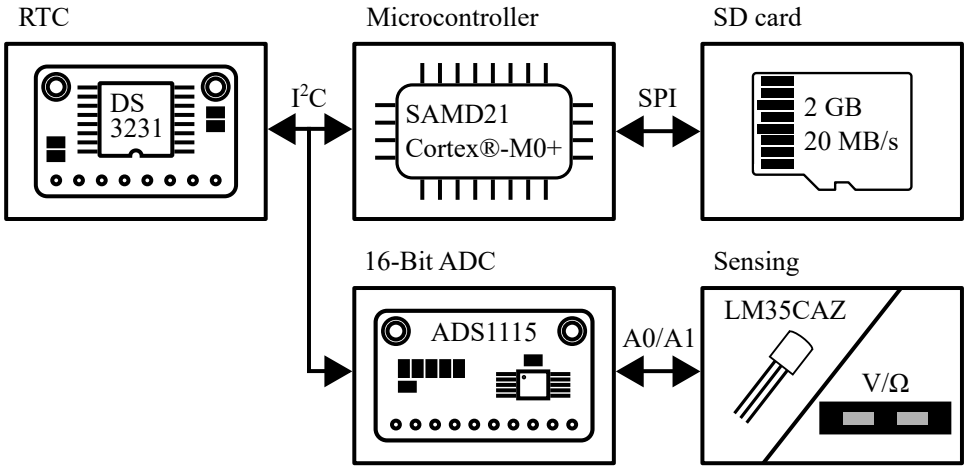

Fig. 2: Master control circuit topology including the communication types between each subsection

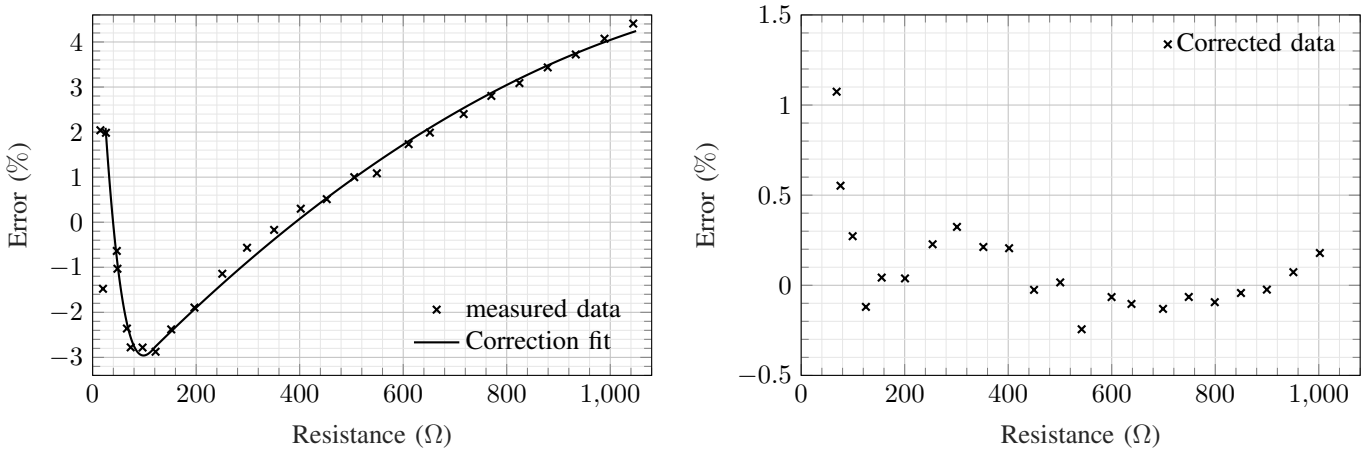

Fig. 3: Error in the initial (left) and the corrected (right) resistance measurements from the Wein-bridge and Peak detector circuitry.

temperature during each measurement [16]. Although other temperature sensors are available, the LM35 can operate at 3.3 V, does not require external capacitors/resistors and only requires 30 μs of power to reach a steady state value.

IV. Battery life

As covered in previous work, turbidity currents are random in nature and there can be many months between events [17]. As such, it is important to ensure that the power consumption of electrical circuit is minimal to ensure the datalogger can measure data during the entire period of a turbidity current [18]. The lifetime of a battery within a circuit can be estimated as:

$$L = 0.7\frac{C}{I} \tag{2}$$

where C is the capacity of the battery and I is the mean current draw. The datalogger is powered using 12 Ansmann AA batteries with a capacity of 2700 mAh [19]. The 12 batteries were arranged in 4 parallel, 3 series to ensure a 4.5 V supply. The supply to the circuit was regulated using an XC6206 3.3 V low drop-out regulator with a quiescent current as low as 1 μA [20]. The current consumption of the datalogger was measured at less than 1 mA on average, as such, the datalogger can record data for up to 315 days.

V. Initial sensor testing and calibration

Before the SSDL was deployed, the accuracy of the circuit was measured from 0 to 1 KΩ using fixed value resistors. Each resistor was measured using the SSDL and was compared against the 4-wire resistance measurement from a Keithley 2410 sourcemeter. The initial measurement error of the Wein-bridge can be seen in Fig. 3. The error in the measured resistance values is less than 4.5% below 1 KΩ. Above 25 Ω, a clear trend can be seen in the measurement error of the sensor. To increase the accuracy of the sensor, a correction factor can be used to scale the measured data. Based on the initial measurements, the correction factor C can be modelled using

$$\begin{aligned} C = &- 5.90 \times 10^{-6}R^3 + 2.23 \times 10^{-3}R^2 \\ &+ 2.71 \times 10^{-1}R + 7.55 \end{aligned} \tag{3}$$

when the measured resistance is less than 120 Ω and

$$C = -4.05 \times 10^{-6}R^2 + 1.23 \times 10^{-2}R - 4.19 \tag{4}$$

when the resistance is greater than 120 Ω. Using Eq. 3 and 4, the measurement error is reduced to less than 0.5% for resistances between 50 and 1000 Ω (Fig. 3). Although there measurement error of the sensor has been reduced, the correction factor is not calibrated from resistances below 50 Ω or above 1 KΩ. To properly calibrate the sensor, the full resistance range of the sensor in saline water should be measured.

A. Saline water testing

To test the salinity response of the conductivity sensor, the sensor head was placed into water samples with salinity concentrations of 0, 5, 10, 15, 20, 25, 30 and 34 g/l. The test was repeated twice in environments with different ambient temperatures. The water, sensing circuitry, and temperature sensor were left undisturbed for approximately 24 hours during each measurement.

The response of the conductivity sensor and the temperature sensor to saline water can be seen in Fig. 4. The data for the conductivity measurements with the temperature sensor outside of the water are not shown as the data for the 25 g/l and 35 g/l are erroneous. The measured resistance of the conductivity sensor changes with the salinity concentration and the temperature. The temperature response of the conductivity probe increases with increasing salinity concentration. The steep temperature increase at the beginning of the measurements for each water sample is an artefact of each water sample being stored at elevated temperatures before measurement. From the data, the measured resistance of the water decreases with increasing salinity concentration and agrees with data published within the literature.

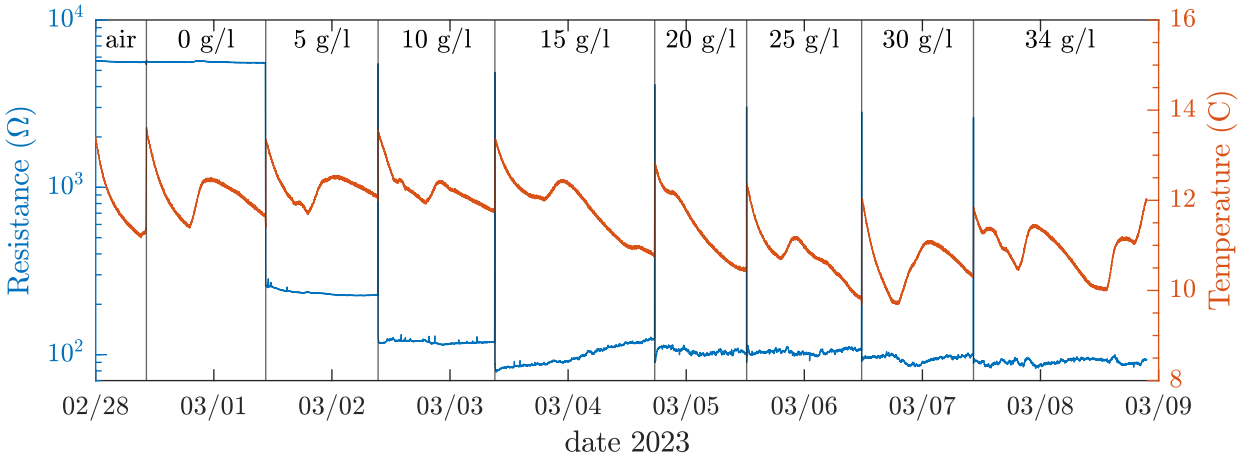

Fig. 4: Measured resistance from the SSDL in air and in different saline solutions with LM35 temperature readings.

The average measured resistance of the conductivity probe in the saline solutions is plotted in Fig. 5. From the data, it can be seen that the average ambient temperature significantly effects the measured resistance of the probe. In high-purity water and air, the measured resistance of the circuit remains stable at 5.6 KΩ and decreases with increasing salinty concentration. The average measured resistance of the saline solutions decreases with decreasing temperature. As the data in Fig. 4 shows that the temperature change does not cause a significant change in the resistance to the degree that is observed in Fig. 5, the change in resistance must be attributed to changes in the driving and sensing circuitry. Further observations of the circuitry have shown that the ambient humidity effects the measured voltage within the sensing circuit and so the circuits should be sealed in future work to correctly calibrate the sensor.

VI. Sensor casing and internal structure

The watertight enclosure, internal frame with PCB, batteries and the sensor head can be seen in Fig. 6. The watertight enclosure used for the turbidity current datalogger was the 2" Type II Anodized 6061-T6 Aluminum watertight enclosure from Blue Robotics [21]. The enclosures come with pre-made double O-ring end caps ensuring the enclosure can withstands depths of up to 950 m. The sensor was made using two high purity (>99.9%) platinum sheets from GoodFellow and have a separation of 1 cm. The platinum electrodes cannot be bonded to directly using conventional soldering and so stranded wires are wrapped around the platinum sheets to make physical contact. The stranded wires and platinum sheets are sealed using two party epoxy that provides a water-tight seal and ensures the stranded wire keeps in physical contact with the platinum. The LM35 is sealed close to the sensor head within the enclosure to minimise thermal lag during measurements. To house the internal electronics and batteries, a mounting structure was fabricated using a 3D-printer that was then constructed using 3 mm threaded rods. Each 3D printed section contained slots for the PCBs and battery holders and each section was fasted in place using 3 mm hex nuts. The SD card was mounted using the SD card holder slot from the microcontroller.

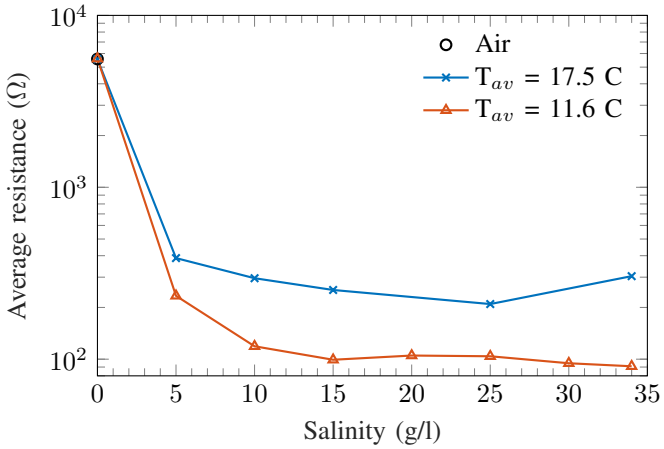

Fig. 5: Comparison of the average salinity resistance with the temperature in and out of the water.

VII. Bute Inlet measurements

The non-cloggable SSDL was deployed in the Bute Inlet, British Columbia, Canada, 15m above the channel floor from the 5th to the 16th of September. The recorded resistance and temperature form the probe is plotted in Fig. 6. From the data, the temperature of the channel floor maintains a steady 7.5 to 8 C. From the 12th to the 16th a clear correlation between the water temperature and the measured resistance can be seen. During the measurements, a clear increase can be seen in the resistance of the water on 5th which lasts until the 9th of September. An optical back-scatter that was deployed with the SSDL has confirmed the influx of a large sediment concentration at these times which correlates to the periods of increased resistance hear. As the SSDL still needs to be calibrated for sediment concentration and temperature, the data here cannot be converted into sediment concentration, although

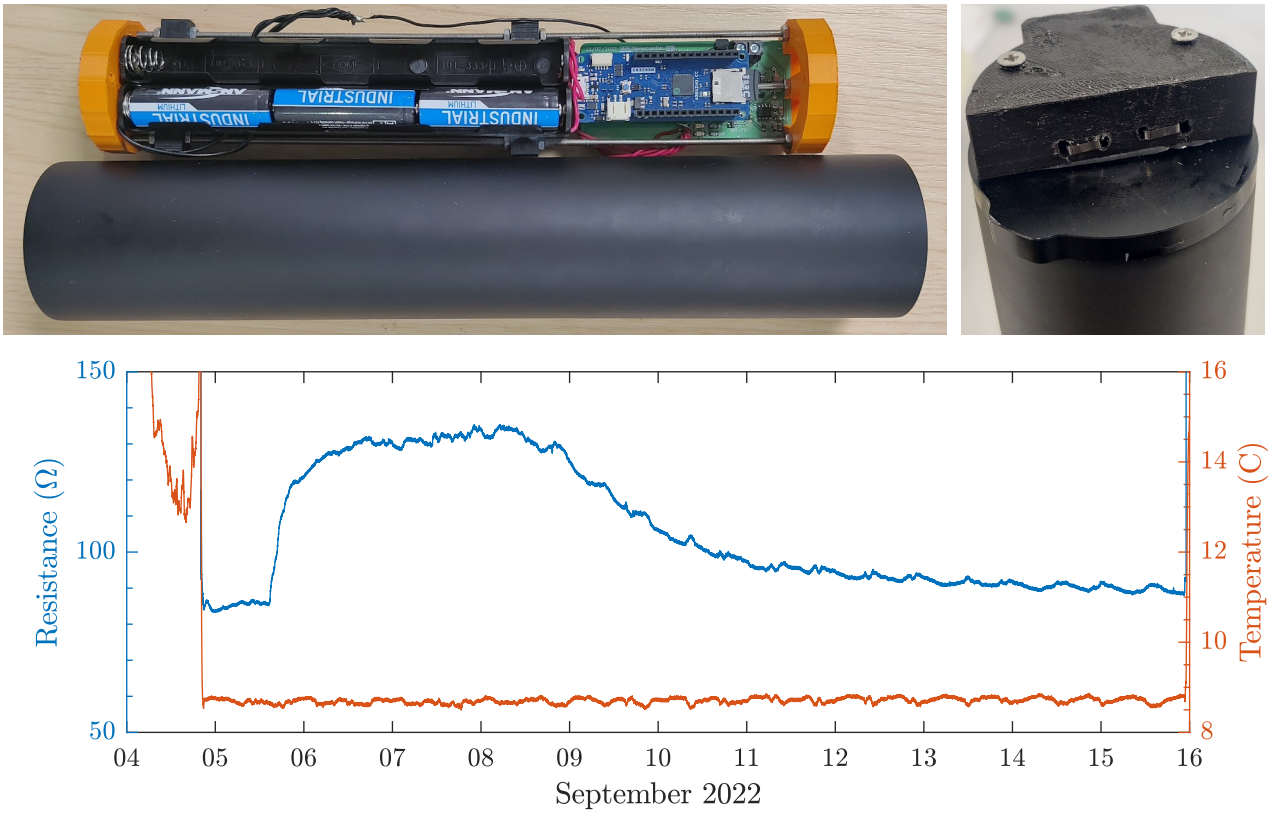

Fig. 6: SSDL casing with internal control circuits and power (left) and the platinum sensor head (right) and the recorded data in the Bute Inlet during the turbidity current (bottom).

it is clear that the sensor is capable of detecting turbidity currents.

VIII. Conclusion

The initial results of a non-cloggable SSDL have been presented. Controlled salinity concentration experiments demonstrate that the SSDL is capable of measuring the changes in salinity concentration and temperature. The salinity concentration measurements have shown that the temperature and humidity must be controlled in order to ensure that the measurements from the sensor head are not affected. The datalogger is capable of measuring water conductivity and temperature once every 4 s for up to 1 year using commercial off-the-shelf AA batteries. This lifetime can be increased by reducing the measurement period.

To house the internal circuitry for seafloor measurements, a 3D printed structure was built to hold the microcontroller and sensor circuitry. After recording data in the Bute Inlet, Canada, the sensor was capable of detecting a turbidity current over the period of 5 days which correlated to an increase in the measured resistance whilst the temperature remained constant. In future work, the sensor will be calibrated against sediment concentration in a temperature controlled environment to ensure that the measured resistance can be converted to sediment concentration.

References

[1] P. J. Talling, R. B. Wynn, D. G. Masson, M. Frenz, B. T. Cronin, R. Schiebel, S. Akhmetzhanov, A. M. Dallmeier-Tiessen, S. Benetti, P. P. E. Weaver, A. Georgiopoulou, C. Zuhlsdorff, and L. A. Amy, "Onset of submarine debris flow deposition far from original giant landslide," *Nature*, vol. 450, no. 7169, pp. 541–544, September 2007, DOI: 10.1038/nature06313.

[2] S. Hage, V. V. Galy, M. J. B. Cartigny, S. Acikalin, M. Clare, D. Grocke, R. G. Hilton, J. E. Hunt, D. G. Lintern, C. A. McGhee, D. R. Parsons, C. D. Stacey, E. J. Simner, and P. J. Talling, "Efficient preservation of young terrestrial organic carbon in sandy turbidity-current deposits," *Geology*, vol. 48, no. 9, pp. 882–887, April 2020, DOI: 10.1130/G47320.1.

[3] A. Ballent, S. Pando, M. Purser, M. F. Juliano, and I. Thomsen, "Modelled transport of benthic marine microplastic pollution in the Nazaré Canyon," *Biogeosciences*, vol. 10, no. 12, pp. 7957–7970, October 2013, DOI: 10.5194/bg-10-7957-2013.

[4] I. A. Kane, M. A. Clare, E. Miramontes, R. Wogelius, J. J. Rothwell, P. Garreau, and F. Pohl, "Seafloor microplastic hotspots controlled by deep-sea circulation," *Science*, vol. 368, no. 6495, pp. 1140–1145, June 2020, DOI: 10.1126/science.aba5899.

[5] L. Carter, R. Gavey, P. J. Talling, and J. T. Liu, "Insights into Submarine Geohazards from Breaks in Subsea Telecommunication Cables," *Oceanography*, vol. 27, no. 2, pp. 58–67, Oct 2015, DOI: 10.5670/oceanog.2014.40.

[6] F. Jourdin, P. R. Renosh, A. A. Charantonis, N. Guillou, S. Thiria, F. Badran, and T. Garlan, "An Observing System Simulation Experiment (OSSE) in Deriving Suspended Sediment Concentrations in the Ocean From MTG/FCI Satellite Sensor," *IEEE Transactions on Geoscience and Remote Sensing*, vol. 59, no. 7, pp. 5423–5433, 2021, DOI: 10.1109/TGRS.2020.3011742.

[7] M. Zeng, J. Peng, L. Jiang, and J. Feng, "Temporal and Spatial Distribution of Suspended Sediment Concentration in Lakes Based on Satellite Remote Sensing and Internet of Things," *IEEE Access*, vol. 9, pp. 87 849–87 856, 2021, DOI: 10.1109/ACCESS.2021.3089367.

[8] W. Liu, Y. Gu, B. Li, and L. Wang, "Enabling Suspended Sediment Concentration Detection With Passive RFID Tags," *IEEE Sensors Journal*, vol. 20, no. 15, pp. 8663–8672, 2020, DOI: 10.1109/JSEN.2020.2983111.

[9] E. F. Eidam, T. Langhorst, E. B. Goldstein, and M. McLean, "OpenOBS: Open-source, low-cost optical backscatter sensors for water quality and

sediment-transport research," *Limnology and Oceanography: Methods*, vol. 20, no. 1, 2022, DOI: 10.1002/lom3.10469.
[10] D. Sehgal, N. Martínez-Carreras, C. Hissler, V. F. Bense, and A. J. F. T. Hoitink, "A Generic Relation Between Turbidity, Suspended Particulate Matter Concentration, and Sediment Characteristics," *Journal of Geophysical Research: Earth Surface*, vol. 127, no. 12, 2022, DOI:10.1029/2022JF006838.
[11] R. Huang and Q. Zhang, "Concentration measurement without calibration of natural sediment particles using backscatter sensing with optical fibres," *Measurement*, vol. 167, p. 108256, 2021, DOI: 10.1016/j.measurement.2020.108256.
[12] T. Lanckriet, J. A. Puleo, and N. Waite, "A Conductivity Concentration Profiler for Sheet Flow Sediment Transport," *IEEE Journal of Oceanic Engineering*, vol. 38, no. 1, pp. 55–70, 2013, DOI: 10.1109/JOE.2012.2222791.
[13] F. Grossmann, D. Hurther, J. van der Zanden, I. Cáceres, A. Sánchez-Arcilla, and J. M. Alsina, "Near-Bed Sediment Transport During Offshore Bar Migration in Large-Scale Experiments," *Journal of Geophysical Research: Oceans*, vol. 127, no. 5, 2022, DOI: 10.1029/2021JC017756.
[14] J. C. Pintado-Patiño, J. A. Puleo, D. Krafft, and A. Torres-Freyermuth, "Hydrodynamics and sediment transport under a dam-break-driven swash: An experimental study," *Coastal Engineering*, vol. 170, 2021, DOI: 10.1016/j.coastaleng.2021.103986.
[15] "MKR Zero - Arm® Cortex®-M0 32-bit SAMD21 processor," docs.arduino.cc/hardware/mkr-zero, accessed: 13/01/2023.
[16] "LM35CAZ/NOPB: ±0.5°C 4V-30V, Temperature sensor with analog output," ti.com/store/ti/en/p/product/?p=LM35CAZ/NOPB, accessed: 16/06/2021.
[17] P. J. Talling, M. L. Baker, E. L. Pope, S. C. Ruffell, R. S. Jacinto, M. S. Heijnen, S. Hage, S. M. Simmons, M. Hasenhündl, C. J. Heerema, C. McGhee, R. Apprioual, A. Ferrant, M. J. B. Cartigny, D. R. Parsons, M. A. Clare, R. M. Tshimanga, M. A. Trigg, C. A. Cula, R. Faria, A. Gaillot, G. Bola, D. Wallance, A. Griffiths, R. Nunny, M. Urlaub, C. Peirce, R. Burnett, J. Neasham, and R. J. Hilton, "Longest sediment flows yet measured show how major rivers connect efficiently to deep sea," *Nature Communications*, vol. 13, 2022, DOI: 10.1038/s41467-022-31689-3.
[18] L. J. Bradley and N. G. Wright, "Optimising SD Saving Events to Maximise Battery Lifetime for Arduino™/Atmega328P Data Loggers," *IEEE Access*, vol. 8, pp. 214 832–214 841, 2020, DOI: 10.1109/ACCESS.2020.3041373.
[19] "Alkaline Manganese (Mercury free) Battery, 1.5 V, AA, 2.7 Ah," farnell.com/ansmann/1502-0006/..., accessed: 12/01/2023.
[20] "XC6206 Series - Low ESR Cap. Compatible Positive Voltage Regulators," torexsemi.com/.../?name=xc6206, accessed: 13/01/2023.
[21] "Blue Robotics - 2", 3" and 4" Watertight Enclosure Tubes," bluerobotics.com/store/watertight-enclosures/..., accessed: 12/01/2023.

Luke J. Bradley is a Research Associate working within the Rolls Royce UTC group at the University of Strathclyde. He received his Bachelor of Engineering in Electrical and Electronic Engineering from Newcastle University in 2015, from which, he worked in the area of Cryogenic Power Electronics and received his PhD from Newcastle University in 2020. His research interests include power electronics and circuits at cryogenic temperatures, power device simulations and microcontroller data logging applications.

Sean C. Ruffell is a marine geophysics postgraduate at Durham University working within the Earth Science department. He received his Master of Science in Geology at the University of Southampton in 2019. Sean's research interests include turbidity currents, geohazards, and the dynamic nature of submarine canyons.

Peter J. Talling is a Professor of Marine Geohazards at Durham University, in a position that is jointly held in the Departments of Earth Sciences and Geography. Over the last decade, he has led a series of international projects that have measured turbidity currents in detail in the oceans for the first time, at a series of sites worldwide. Most recently he led work that remotely sensing a turbidity current that travelled for 1,100 km offshore from the mouth of the Congo River, at speeds of 5 to 8 m/s.

Nick G. Wright is a Professor of Electronic Materials at Newcastle University UK and a Fellow of the Turing Institute. He received his Bachelor and PhD degrees from Edinburgh University. He has led major projects on power semiconductor devices, robotics and AI. He has authored over 200 papers, contributed to over 10 patents and made numerous conference presentations. His research interests include electronic materials, power devices, and the applications of materials to robotics and artificial intelligence – particularly for manufacturing and deep ocean exploration.